

# Lyapunov Stability-Aware Stackelberg Game for Low-Altitude Economy: A Control-Oriented Pruning-Based DRL Approach

Yue Zhong, Jiawen Kang\*, Yongju Tong, Hong-Ning Dai, Dong In Kim, *Fellow, IEEE*,  
 Abbas Jamalipour, *Fellow, IEEE*, Shengli Xie, *Fellow, IEEE*

**Abstract**—With the rapid expansion of the low-altitude economy, Unmanned Aerial Vehicles (UAVs) serve as pivotal aerial base stations supporting diverse services from users, ranging from latency-sensitive critical missions to bandwidth-intensive data streaming. However, the efficacy of such heterogeneous networks is often compromised by the conflict between limited onboard resources and stringent stability requirements. Moving beyond traditional throughput-centric designs, we propose a Sensing–Communication–Computing–Control (SC<sup>3</sup>) closed-loop framework that explicitly models the impact of communication latency on physical control stability. To guarantee mission reliability, we leverage the Lyapunov stability theory to derive an intrinsic mapping between the state evolution of the control system and communication constraints, transforming abstract stability requirements into quantifiable resource boundaries. Then, we formulate the resource allocation problem as a Stackelberg game, where UAVs (as leaders) dynamically price resources to balance load and ensure stability, while users (as followers) optimize requests based on service urgency. Furthermore, addressing the prohibitive computational overhead of standard Deep Reinforcement Learning (DRL) on energy-constrained edge platforms, we propose a novel and lightweight pruning-based Proximal Policy Optimization (PPO) algorithm. By integrating a dynamic structured pruning mechanism, the proposed algorithm significantly compresses the neural network scale during training, enabling the UAV to rapidly approximate the game equilibrium with minimal inference latency. Simulation results demonstrate that the proposed scheme effectively secures control loop stability while maximizing system utility in dynamic low-altitude environments.

**Index Terms**—Sensing–Communication–Computing–Control (SC<sup>3</sup>) closed-loop, Low-altitude economy, Lyapunov stability theory, Stackelberg game, Pruning-based PPO algorithm.

## I. INTRODUCTION

With the strategic expansion of the Low-Altitude Economy (LAE), Unmanned Aerial Vehicles (UAVs) are rapidly evolving from simple sensing platforms into autonomous mobile

Yue Zhong, Jiawen Kang, Yongju Tong, and Shengli Xie are with the School of Automation, Guangdong University of Technology, Guangzhou 510006, China (e-mail: 2112404106@mail2.gdut.edu.cn; kavinkang@gdut.edu.cn; tongyongju1@mails.gdut.edu.cn; shlxie@gdut.edu.cn).

Hong-Ning Dai is with the Department of Computer Science, Hong Kong Baptist University, Hong Kong, China (e-mail: hndai@ieee.org).

Dong In Kim is with the Department of Electrical and Computer Engineering, Sungkyunkwan University, Suwon 16419, South Korea (e-mail: dongin@skku.edu).

Abbas Jamalipour is with the School of Electrical and Computer Engineering, University of Sydney, Australia, and with the Graduate School of Information Sciences, Tohoku University, Japan (e-mail: a.jamalipour@ieee.org).

(\*Corresponding author: Jiawen Kang)

agents capable of executing complex tasks in high-density airspace [1]. Within this heterogeneous landscape, UAVs are required to concurrently support a wide spectrum of service demands, ranging from throughput-oriented applications (e.g., high-definition video streaming for large-scale gatherings) to urgency-sensitive tasks that demand ultra-reliable and low-latency control signaling (e.g., emergency response and control signaling). Among these scenarios, post-disaster emergency response stands out as a critical and challenging subset of the LAE, imposing stringent requirements on system robustness. In these safety-critical missions, where ground infrastructure is often paralyzed, UAVs serve not only as aerial communication relays but also as dynamic control nodes essential for restoring information-physical links [2]. Under strict energy and bandwidth constraints, the contention for communication resources inevitably induces latency, which degrades the performance of the networked control system [3].

Unlike traditional networks focused on throughput performance, the LAE between UAVs and users is inherently a closed-loop process comprising Sensing, Communication, Computing, and Control (SC<sup>3</sup>) [4]. The effectiveness and reliability of tasks depend on the end-to-end SC<sup>3</sup> latency [5], where fluctuations in communication resources propagate through the loop, degrading physical control stability. Specifically, the loop latency caused by: i) *Sensing latency* is time for user devices to detect environmental changes and generate signals; ii) *Communication latency* is Air-to-Ground (A2G) link latency subject to channel interference; iii) *Computing latency* is latency for encoding, decoding, and priority scheduling; and iv) *Control latency* is the feedback delay in UAV decision-making. Within this loop, the UAV’s state evolution (e.g., position, rotation, and velocity) depends on the timely reception of control commands. Delays exceeding the control period induce input lag and state errors, potentially leading to mission failure [4]. Consequently, resource allocation is no longer a purely valid communication problem but a control-communication co-design problem [6]. To address this issue, we apply the Lyapunov stability theory to model the dynamics of UAV state updates [7]. By establishing a Lyapunov function for error states, we transform abstract physical stability requirements into quantifiable communication latency boundaries, providing a rigorous basis for control-aware resource allocation.

Given scarce LAE resources and heterogeneous user bandwidth demands, we model resource regulation as a Stackelberg game [8]. UAVs, functioning as the leaders, dynamically set

resource prices to regulate the network load, thereby maintaining the system within its stable operating region [9]. Users, serving as followers, optimize their resource requests based on service urgency and pricing. This game-theoretic framework facilitates load balancing and acts as a distributed control mechanism, i.e., urgency-sensitive users pay a premium for priority, while non-urgent users access the network at lower costs, thereby stabilizing the closed-loop control system under dynamic loads. However, solving the Stackelberg equilibrium in real-time is challenging due to the time-varying environment and incomplete information regarding user utilities, while Deep Reinforcement Learning (DRL) offers a paradigm for decision-making under uncertainty [10], in which traditional models like Proximal Policy Optimization (PPO) involve massive parameters [11]. For battery-powered UAVs already burdened with communication and control tasks, executing heavy neural networks introduces unacceptable computation latency, undermining the  $SC^3$  loop stability. To resolve this conflict, we design a lightweight pruning-based PPO algorithm utilizing dynamic structured pruning. By iteratively removing redundant neurons during training, it compresses the network without accuracy loss, enabling rapid edge learning of optimal pricing strategies on UAVs. The main contributions of this paper are summarized as follows.

- We construct a unified Sensing, Communication, Computing, and Control ( $SC^3$ ) closed-loop framework specifically tailored for the heterogeneous LAE. By explicitly modeling the coupling mechanism wherein communication resource fluctuations propagate through end-to-end latency, we quantify the impact of information transmission delays on the real-time responsiveness and physical stability of the control loop.
- To rigorously guarantee the system stability identified in our framework, we derive an intrinsic mapping between control dynamics and network constraints via the Lyapunov stability theory. This theoretical transformation converts abstract stability requirements into explicit communication latency boundaries. Based on these constraints, we formulate a Stackelberg game between UAVs and users. This formulation utilizes an incentive-based pricing mechanism to balance heterogeneous user demands and limited UAV resources, ensuring system stability under dynamic loads.
- To address the prohibitive computational overhead of solving the game on energy-constrained UAVs, we propose a novel pruning-based PPO algorithm incorporating dynamic structured pruning. This approach significantly reduces the inference latency and energy consumption of the control policy, enabling the UAV to rapidly approximate the Stackelberg equilibrium and maintain robust operation within the  $SC^3$  loop.

The remainder of this paper is organized as follows. Section II provides a comprehensive review of the related literature. Section III establishes the system architecture and the  $SC^3$  closed-loop framework, formally defining the optimization problem and modeling the interaction between the UAV and users as a Stackelberg game. To solve this formula-

tion, Section IV proposes the pruning-based PPO algorithm designed to efficiently approximate the game equilibrium. Section V presents and analyzes the numerical simulation results, and Section VI concludes the paper.

## II. RELATED WORK

### A. Service Provisioning and Mission Planning in LAE

With the rapid development of the LAE, UAVs are regarded as aerial base stations for flexible connectivity and service provisioning. Existing studies primarily focused on deployment and service optimization from networking perspectives. In [12], the authors proposed a DRL-based LAE framework that jointly optimizes base station beamforming and UAV trajectories to improve communication sum-rate under sensing and flight constraints. In [13], the authors proposed a digital twin-enabled multi-agent LAE framework where UAVs act as Mobile Edge Computing (MEC) servers for vehicular task offloading, and achieve lower average service delay via a Multi-Agent Deep Q-Network (MADQN) algorithm. Public safety represents a critical area within the LAE, where UAV-assisted emergency response is essential when disasters damage ground infrastructure. In [14], the authors designed a two-phase multiobjective trajectory optimization scheme for first-aid supply delivery to reduce computational time under priority constraints. In [15], the authors proposed a swarm intelligence-based method for constrained multi-objective UAV 3-D path planning, jointly optimizing flight distance and terrain threat to enhance emergency response efficiency and safety. Despite these advancements, a fundamental disconnect remains, i.e., most works treat communication resource allocation and UAV physical control as decoupled entities. Few studies integrate sensing delays, computing latency, and physical state dynamics (e.g., stability) into a unified closed-loop model. This paper bridges this gap by introducing Lyapunov stability analysis to explicitly couple physical-layer control performance with logical-layer communication resource allocation.

### B. Incentive Mechanism for LAE

Given the limited resources (e.g., spectrum, power, and computing capability) of UAVs in LAE, effective incentive mechanisms are essential to coordinate resource competition and ensure different service provisioning. In [16], the authors designed an Age of Information (AoI)-aware UAV-assisted crowdsensing framework and applied contract theory to design optimal contracts under information asymmetry, maximizing platform utility and data freshness. In [17], the authors proposed a Stackelberg game-based spectrum trading framework for UAV swarms, where UAV-to-base station links act as leaders to set trading prices and allocate resources, incentivizing UAV-to-UAV links to share spectrum and improving system utility under interference-aware access. In [18], the authors investigated post-disaster rescue in aerial-ground UAV networks and jointly optimized task offloading and resource allocation to reduce service latency. Nevertheless, these studies predominantly optimize resources from purely networking or economic perspectives (e.g., maximizing throughput or utility),

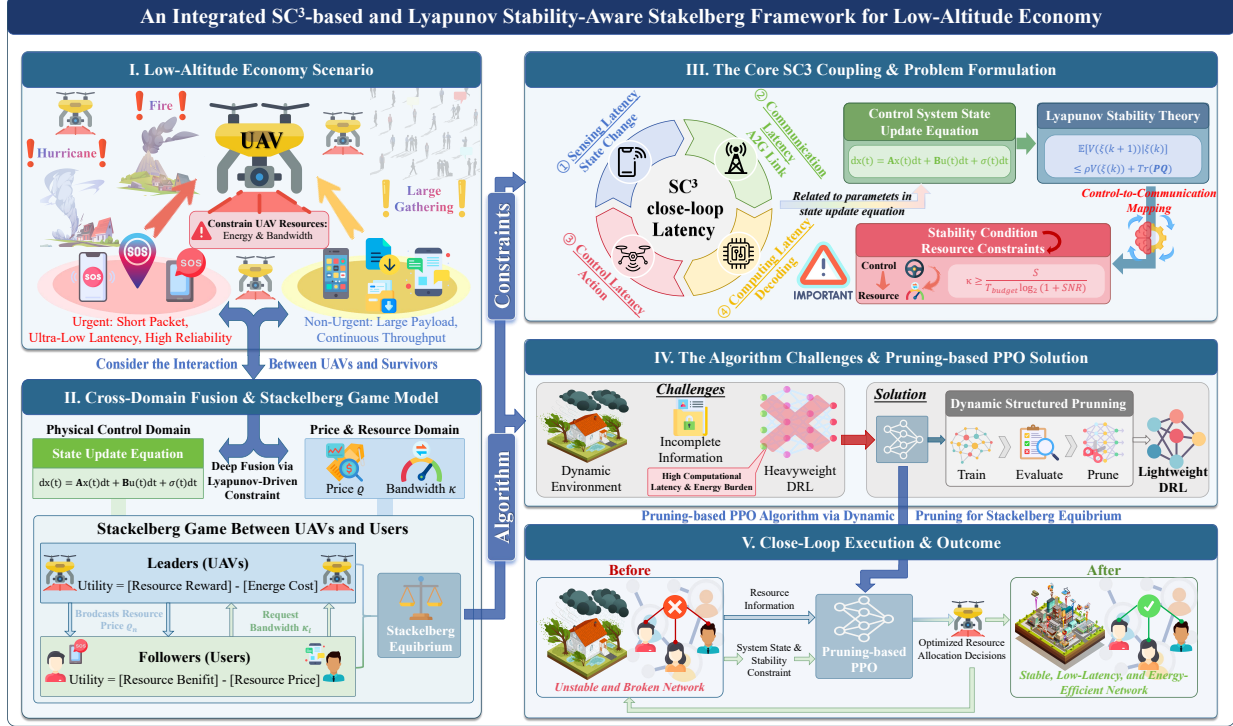


Fig. 1: Illustration of the integrated  $SC^3$ -based and Lyapunov stability-aware Stackelberg solved by lightweight pruning-based MADRL for the low-altitude economy framework. The framework illustrates the integration of heterogeneous user demands, the Lyapunov-driven fusion of  $SC^3$  dynamics, and the Stackelberg game formulation, ultimately solved by the dynamic structured pruning-based PPO algorithm.

largely overlooking the underlying closed-loop control dynamics. Consequently, current incentive designs lack a mechanism to couple pricing strategies with physical safety margins. In contrast, our paper proposes a novel Stackelberg game explicitly driven by Lyapunov stability theory [19]. Here, the leader's pricing strategy is determined not merely by resource scarcity but intrinsically by the system's control stability state. This formulation ensures that the game equilibrium guarantees physical system robustness alongside economic balance, a cross-domain perspective that remains unexplored in existing LAE research.

#### C. Pruning-based DRL Algorithm

While DRL is effective for high-dimensional resource optimization, the massive parameter size of traditional deep networks often incurs prohibitive computation and energy overheads on resource-constrained UAV platforms. To address this challenge, model pruning has been introduced to enable “Tiny-DRL”, offering a practical solution for edge intelligence. For example, the authors in [8] proposed a pruning-based multi-agent DRL framework for UAV-twin migration, significantly reducing the actor-critic model size while preserving decision-making performance. Similarly, the authors in [20] designed a pruning-based method for dependency-aware MEC offloading, filtering low-probability actions during training to accelerate convergence. Pruning techniques are generally categorized into unstructured pruning [21] and structured pruning [22]. Unstructured pruning creates sparse networks by removing individual weights, but the resulting irregular sparsity is often difficult to accelerate on standard hardware,

limiting its practical utility for real-time control. Conversely, structured pruning eliminates entire geometric structures, producing compact architectures that are hardware-friendly and offer predictable latency reductions. Therefore, this paper adopts dynamic structured pruning to achieve flexible, reliable, and lightweight learning, ensuring the algorithm meets the stringent timing constraints of the UAV control loop.

### III. SYSTEM MODEL AND PROBLEM FORMULATION

We consider an LAE scenario where terrestrial infrastructure is paralyzed, and a fleet of UAVs is deployed as aerial base stations to restore connectivity [23]. As illustrated in Fig. 1, the proposed framework presents an integrated architecture for UAV-assisted communications within the LAE. It begins by characterizing heterogeneous service demands, ranging from urgency-sensitive emergency response to throughput-oriented coverage for large gatherings, under strict UAV energy and bandwidth constraints. To align physical control with information transmission, the framework establishes an  $SC^3$  closed-loop, using Lyapunov stability theory to map control stability requirements into explicit communication latency bounds. These constraints drive a Stackelberg game for optimal resource allocation, which is solved by a lightweight pruning-based PPO algorithm equipped with dynamic structured pruning. We consider a system comprising a set of UAVs, denoted by  $\mathcal{N} = \{1, \dots, N\}$ , and a set of users, denoted by  $\mathcal{I} = \{1, \dots, I\}$ , who are equipped with mobile sensing devices [24]. This interaction constitutes a closed-loop control system, i.e., UAVs adjust trajectories based on real-time feedback, while users require bandwidth to transmit status updates. To

coordinate this resource-constrained interaction, we formulate a Stackelberg game where UAVs (as leaders) optimize pricing strategies and users (as followers) optimize resource requests, thereby ensuring efficient and stable rescue operations [9].

#### A. Control Model and Latency Model

This subsection presents the formulation of the UAV control dynamics and the end-to-end latency model characterizing the interaction between UAVs and users.

1) *Control Model*: To ensure effective tracking, we model the coupling between physical motion and information latency using a time-triggered architecture with a constant sampling period  $e_n$ . This fixed-period assumption is consistent with the operational constraints of onboard digital flight controllers, which require a synchronized, periodic clock for stable feedback loops [25]. Each period is partitioned into the end-to-end SC<sup>3</sup> latency  $T_n(k)$  (detailed in Section III-A2) and the effective execution window  $\bar{e}_n(k)$ , formulated as  $e_n = \bar{e}_n(k) + T_n(k)$ . Consequently, latency fluctuations inversely modulate the actuation time. Specifically, increasing  $T_n(k)$  compresses the execution window  $\bar{e}_n(k)$ , thereby degrading tracking performance and system stability, where  $k = \{1, 2, \dots, K\}$  is the discrete-time index. Notably, a longer feedback latency  $T_n(k)$  compresses the execution window  $\bar{e}_n(k)$ , thereby degrading the control performance.

Let  $P_n(k), P_i(k) \in \mathbb{R}^3$  denote the 3D positions and  $v_n(k), v_i(k) \in \mathbb{R}^3$  denote the velocities of UAV  $n$  and user  $i$ , respectively [5]. We define the relative state vector as  $x_n(k) = [P_n(k) - P_i(k), v_n(k) - v_i(k)]^T \in \mathbb{R}^6$ . The position of UAV  $n$  and user  $i$  at time index  $k$  are denoted as  $P_n(k) = [x_n(k), y_n(k), z_n]^T$  and  $P_i(k) = [x_i(k), y_i(k), 0]^T$ , respectively. Considering that the UAV typically maintains a constant mission altitude  $z_n$  to ensure communication coverage and flight safety, the primary control objective is to eliminate the horizontal tracking error. Specifically, the controller aims to regulate the UAV's planar coordinates to align with the user's location, i.e.,  $[x_n(k) - x_i(k), y_n(k) - y_i(k)]^T \rightarrow \mathbf{0}$ . The continuous-time evolution of the system is governed by the linear time-invariant stochastic differential equation, which is denoted as [25]

$$dx_n(t) = \mathbf{A}x_n(t)dt + \mathbf{B}u_n(t)dt + \sigma_n(t)dt, \quad (1)$$

where  $\mathbf{A} \in \mathbb{R}^{6 \times 6}$  and  $\mathbf{B} \in \mathbb{R}^{6 \times 3}$  are system matrices determined by the physical constraints and UAV dynamics.  $u_n(t)$  is the control input (e.g., acceleration command), and  $\sigma_n \sim \mathcal{N}(0, \mathbf{Q}_n)$  represents additive white Gaussian noise.

Considering that the UAV maintains the previous command  $u_n(k-1)$  until the new command  $u_n(k)$  is received at time index  $k$ , the discrete-time state update can be derived by integrating Eq. (1) over one sampling interval [26]

$$x_n(k+1) = \Psi_n(k)x_n(k) + \Phi_n^0(k)u_n(k) + \Phi_n^1(k)u_n(k-1) + \sigma_n(k), \quad (2)$$

where  $\Psi_n(k) = e^{\mathbf{A}e_n(k)}$  represents the natural state transition. The input matrices  $\Phi_n^0(k) = \int_0^{\bar{e}_n(k)} e^{\mathbf{A}t} \mathbf{B} dt$  and  $\Phi_n^1(k) = \int_{\bar{e}_n(k)}^{e_n} e^{\mathbf{A}t} \mathbf{B} dt$  characterize the impact of the current and delayed control inputs, respectively [27].

To facilitate the stability analysis, we define an augmented state vector  $\zeta_n(k) = [x_n(k), u_n(k-1)]^T \in \mathbb{R}^9$ . The augmented dynamics can be reformulated as

$$\zeta_n(k+1) = \Psi_n^d(k)\zeta_n(k) + \Phi_n^d(k) + \sigma_n^d(k), \quad (3)$$

where  $\Psi_n^d(k) = \begin{bmatrix} \Psi_n(k) & \Phi_n^1(k) \\ \mathbf{0}_{3 \times 6} & \mathbf{0}_{3 \times 3} \end{bmatrix}$ ,  $\Phi_n^d(k) = \begin{bmatrix} \Phi_n^0(k) \\ \mathbf{I}_{3 \times 3} \end{bmatrix}$ , and  $\sigma_n^d(k) = \begin{bmatrix} \sigma_n(k) \\ \mathbf{0}_{3 \times 1} \end{bmatrix}$ . In practical search scenarios, data packets may be lost due to fading or interference. We introduce a binary variable  $\alpha \in \{0, 1\}$  to model the transmission success (i.e.,  $\alpha = 1$  for success, otherwise  $\alpha = 0$ ). In the event of failure, the UAV fails to update its command and continues to execute the previous action under an open-loop evolution. Therefore, we can reconstruct Eq.(3) as [25]

$$\zeta_n(k+1) = \begin{cases} \Psi_n^d(k)\zeta_n(k) + \Phi_n^d(k)u_n(k) + \sigma_n^d(k), & \alpha = 1, \\ \Psi_n^h(k)\zeta_n(k) + \sigma_n^d(k), & \alpha = 0, \end{cases} \quad (4)$$

where  $\Psi_n^h(k) = \begin{bmatrix} \Psi_n(k) & \Phi_n(k) \\ \mathbf{0}_{3 \times 6} & \mathbf{I}_{3 \times 3} \end{bmatrix}$  with  $\Phi_n(k) = \mathbf{B} \int_0^{e_n(k)} e^{\mathbf{A}t} dt$  representing the free-running dynamics under the old command. Assuming a linear feedback control law  $u_n(k) = \mathbf{K}_n \zeta_n(k)$ , where  $\mathbf{K}_n$  is the control gain matrix [28], we can obtain

$$\zeta_n(k+1) = \begin{cases} \Psi_{cl}^d(k)\zeta_n(k) + \sigma_n^d(k), & \alpha = 1, \\ \Psi_{op}^h(k)\zeta_n(k) + \sigma_n^d(k), & \alpha = 0, \end{cases} \quad (5)$$

where  $\Psi_n^{cl} = \Psi_n^d(k) + \Phi_n^d(k)\mathbf{K}_n$  and  $\Psi_n^{op} = \Psi_n^h(k)$  denote the closed-loop and open-loop transition matrices, respectively.

To ensure the asymptotic stability of the networked control system, we employ the Lyapunov stability theory [29]. We define a quadratic Lyapunov function as  $V_n(\zeta_n(k)) = \zeta_n(k)^T \mathbf{P}_n \zeta_n(k)$ , where  $\mathbf{P}_n$  is a positive definite weighting matrix. To guarantee that the system state converges toward the target, the Lyapunov-like function must satisfy the following descent condition with a decay rate  $\rho_n \in (0, 1)$  [29], i.e.,

$$\mathbb{E}[V_n(\zeta_n(k+1))|\zeta_n(k)] \leq \rho_n V_n(\zeta_n(k)) + \text{Tr}(\mathbf{P}_n \mathbf{Q}_n). \quad (6)$$

2) *Latency Model*: To capture the coupled effects of communication and control, we characterize the end-to-end latency  $T_{i,n}^{total}$  for each user-UAV pair. This latency is decomposed into four primary components, i.e., sensing, communication, computing, and control actuation [5].

The sensing process is initiated when user  $i$  detects a state change, such as the position change [30]. The mobile device's GNSS module identifies the new coordinates, incurring a sensing latency  $T_i^{\text{sense}}$ , which is expressed as

$$T_i^{\text{sense}} = T_i^{\text{pos}} + T_i^{\text{read}}, \quad \forall i \in \mathcal{I}, \quad (7)$$

where  $T_i^{\text{pos}}$  denotes the positioning time of the user's mobile device, the time it takes for the GPS module to successfully determine the location from startup, and  $T_i^{\text{read}}$  represents the I/O latency for the CPU to retrieve data from the hardware buffer [31]. The term  $T_i^{\text{read}}$  is typically of the order of milliseconds, and  $T_i^{\text{pos}}$  depends on the satellite signal strength and the module's warm-start capabilities.

Communication latency represents the uplink transmission latency of the state packet. Based on the Shannon theorem, the transmission time is given by

$$T_{i,n}^{\text{comm}} = \frac{S_i}{R_{i,n}}, \forall i \in \mathcal{I}, n \in \mathcal{N}, \quad (8)$$

where  $R_{i,n} = B_{i,n} \log_2 \left(1 + \frac{w_i h_{i,n}}{\sigma^2}\right)$  is the achievable data rate [32]. The term  $w_i$  represents the transmit power and  $\sigma^2$  is the additive white Gaussian noise [8]. The term  $h_{i,n} = h_0 d_{i,n}^{-\alpha}$  represents the uplink channel gain, which mainly depends on the distance and can be modeled using the free-space path loss model. Moreover,  $h_0$  is the reference gain,  $d_{i,n} = \|P_n - P_i\|$  is the Euclidean distance, and  $\alpha$  is the path loss exponent.

The computing latency  $T_{i,n}^{\text{compute}}$  accounts for data preprocessing at the user side and command generation at the UAV side. For the users, the calculation time includes the time for calculating distances and packaging data packets. For the UAVs, it includes delays for parsing data packets, updating estimates of the user's location, path planning, and generating control commands. It is modeled as

$$T_{i,n}^{\text{compute}} = T_i^{\text{comp}} + T_n^{\text{base}} + \frac{S_i f_0}{f_n}, \forall i \in \mathcal{I}, n \in \mathcal{N}, \quad (9)$$

where  $T_i^{\text{comp}}$  represents the computation latency of the mobile device, which calculates the distance between the current location and the last transmitted location [33]. If the distance exceeds a threshold, the data is packaged. At the UAV side,  $T_n^{\text{base}}$  represents the fixed time for packet decapsulation and state estimation, while the term  $S_i f_0 / f_n$  characterizes the task-specific processing latency, where  $S_i$  is the data size,  $f_0$  is the required CPU cycles per bit and  $f_n$  is the computational frequency of UAV  $n$  [33].

Once the command  $u_n(k)$  is generated, the UAV's flight control system and physical actuators (i.e., the motors and propellers) require time to track the new velocity or acceleration. Assuming a first-order response model for the UAV's propulsion system [34], the response latency  $T_n^{\text{control}}$  is approximated as

$$T_n^{\text{control}} = 4\mu_n, \forall n \in \mathcal{N}, \quad (10)$$

where  $\mu_n$  represents the intrinsic time constant, which is determined by the physical parameters of the UAV.

**Proof.** Consider the UAV's velocity tracking as a first-order system. Let  $V_{\text{cmd}}$  be the target velocity command and  $V_{\text{actual}}(t)$  be the instantaneous velocity at time  $t$ . The dynamic response can be governed by the following first-order ordinary differential equation as

$$\frac{dV_{\text{actual}}(t)}{dt} = x(V_{\text{cmd}} - V_{\text{actual}}(t)), \quad (11)$$

where  $x$  is the gain constant representing the responsiveness of the motor-rotor system. By defining the time constant  $\mu_n = 1/x$ , Eq. (11) is reformulated as  $\mu_n \frac{dV_{\text{actual}}(t)}{dt} + V_{\text{actual}}(t) = V_{\text{cmd}}$ . Given a step command where the desired velocity changes from an initial  $V_0$  to  $V_{\text{cmd}}$  at  $t = 0$ , the analytical solution for  $V_{\text{actual}}(t)$  is obtained as

$$V_{\text{actual}}(t) = V_{\text{cmd}} + (V_0 - V_{\text{cmd}}) e^{-\frac{t}{\mu_n}}. \quad (12)$$

To ensure that the UAV effectively executes the command, we define the control latency  $T_n^{\text{control}}$  as the time at which the velocity error decays to within 2% of its initial step magnitude. Let  $\epsilon(t) = |V_{\text{actual}}(t) - V_{\text{cmd}}|$  be the tracking error [35]. Based on Eq. (12), the error evolution is expressed as

$$\epsilon(t) = |V_0 - V_{\text{cmd}}| e^{-\frac{t}{\mu_n}}. \quad (13)$$

With the settling-time constraint  $\epsilon(T_n^{\text{control}}) \leq 0.02|V_0 - V_{\text{cmd}}|$  in place, we obtain  $e^{-\frac{T_n^{\text{control}}}{\mu_n}} \leq 0.02$ . Consequently, by taking the natural logarithm on both sides, we can obtain

$$T_n^{\text{control}} \geq -\mu_n \ln(0.02) \approx 3.912\mu_n. \quad (14)$$

For engineering tractability in discrete-time control, we approximate this interval as  $T_n^{\text{control}} \approx 4\mu_n$ . This approximation ensures that the UAV's physical state has converged to 98% of the commanded value within one control cycle.  $\square$

Considering the above analysis of latency, we can get the total end-to-end latency from user  $i$  to UAV  $n$ , which is represented as  $T_{i,n}^{\text{total}} = T_i^{\text{sense}} + T_i^{\text{comp}} + T_n^{\text{base}} + \frac{S_i f_0}{f_n} + \frac{S_i}{R_{i,n}} + 4\mu_n$ . In a multi-user scenario where UAV  $n$  interacts with a set of users  $\mathcal{M}_n$ , the effective control latency is bottlenecked by the most delayed information. Therefore, the aggregate latency for UAV  $n$  is defined as the maximum latency among its connected users, i.e.,

$$T_n = \max_{i \in \mathcal{M}_n} \{T_{i,n}^{\text{total}}\}, \forall n \in \mathcal{N}. \quad (15)$$

### B. Stackelberg Game Between UAVs and Users

Given the inherent leader-follower hierarchy in LAE networks, where UAVs possess the authority to allocate spectrum resources while users selfishly compete for optimal service quality, a Stackelberg game formulation is uniquely suited to capture this sequential decision-making process. Accordingly, to optimize resource distribution while ensuring system stability, we model the interaction between UAVs and users as a Stackelberg game. In this hierarchical framework, each UAV  $n$  acts as a leader, determining the bandwidth price  $\varrho_n$  to manage demand and maximize utility [8]. Subsequently, each user  $i$  acts as a follower, deciding the required bandwidth  $\kappa_i$  based on the observed price.

1) *Utilities of UAVs:* The objective of UAV  $n$  is to maximize its revenue from bandwidth provisioning while accounting for the operational cost  $c_n$ . The utility function of UAV  $n$  is defined as [8]

$$U_n^L = \sum_{i \in \mathcal{M}_n} \beta_{i,n} (\varrho_n - c_n) \kappa_i, \forall n \in \mathcal{N}, \quad (16)$$

where  $c_n$  is the bandwidth cost,  $\beta_{i,n} \in \{0, 1\}$  is a binary variable, when  $\beta_{i,n} = 1$  indicates that UAV  $n$  is associated with user  $i$ . Therefore, the optimization problem of the UAV (i.e., the leader) is formulated as follows:

$$\begin{aligned} \text{Problem 1 : } \max_{\varrho_n} U_n^L &= \sum_{i \in \mathcal{M}_n} \beta_{i,n} (\varrho_n - c_n) \kappa_i, \\ \text{s.t. } \mathbb{E}[V_n(\zeta_n(k+1)) | \zeta_n(k)] &\leq \rho_n V_n(\zeta_n(k)) + \text{Tr}(\mathbf{P}_n \mathbf{Q}_n), \end{aligned} \quad (17a)$$

$$\sum_{i \in \mathcal{M}_n} \kappa_i \leq \kappa_n^{\text{total}}, \quad (17b)$$

Constraint (17a) guarantees probabilistic tracking stability by the Lyapunov requirement, and (17b) imposes capacity limits. It is noted that the price  $\varrho_n$  serves as a virtual incentive signal rather than a financial cost, functioning to prioritize resource allocation for users with higher urgency weights  $\vartheta_i$ .

**Proposition 1. (Control-to-Communication Mapping):** *To satisfy the stability condition that is defined in (17a) with a decay rate  $\rho_n$ , the minimum bandwidth  $\kappa_i^{\min}$  required for user  $i$  is given by*

$$\kappa_i^{\min} = \frac{S_i}{T_{\text{budget}} \log_2(1 + \text{SNR}_{i,n})}, \quad (18)$$

where  $T_{\text{budget}}$  is the allowable communication latency margin, and  $\text{SNR}_{i,n} = \frac{P_i h_0 d_{i,n}^{-\alpha}}{\sigma^2}$  denotes the signal-to-noise ratio (SNR) from user  $i$  to UAV  $n$  [32].

**Proof.** Let  $\xi_{i,n}$  be the probability of successful transmission from user  $i$  to UAV  $n$ . The expectation in (17a) can be expanded as

$$\xi_{i,n} V_{\text{close}} + (1 - \xi_{i,n}) V_{\text{open}} \leq \rho_n V_{\text{current}} + \text{Tr}(\mathbf{P}_n \mathbf{Q}_n), \quad (19)$$

where  $V_{\text{close}}(\zeta_k) = \zeta_n(k)^T \Psi_{cl}^T \mathbf{P}_n \Psi_{cl} \zeta_n(k)$ ,  $V_{\text{open}} = \zeta_n(k)^T \Psi_{op}^T \mathbf{P}_n \Psi_{op} \zeta_n(k)$ , and  $V_{\text{current}} = \rho_n \zeta_n(k)^T \mathbf{P}_n \zeta_n(k)$ . Solving for  $\xi_{i,n}$  yields the minimum success probability threshold  $\Gamma_n$ , expressed as

$$\xi_{i,n} \geq \frac{V_{\text{open}} - \rho_n V_{\text{current}} - \text{Tr}(\mathbf{P}_n \mathbf{Q}_n)}{V_{\text{open}} - V_{\text{close}}} \triangleq \Gamma_n. \quad (20)$$

The Lyapunov constraint specifies a success probability of  $P(T_n \leq e_n) \geq \Gamma_n$  and a failure probability of  $P(T_n \geq e_n) \leq 1 - \Gamma_n$ . By invoking Markov's Inequality [36], the tail probability of the total latency  $T_n$  exceeding the sampling period  $e_n$  is bounded by  $P(T_n \geq e_n) \leq \mathbb{E}[T_n]/e_n$ . To ensure  $P(T_n \leq e_n) \geq \Gamma_n$ , we require  $\mathbb{E}[T]/e_n \leq 1 - \Gamma_n$ , i.e.,  $\mathbb{E}[T_n] \leq (1 - \Gamma_n)e_n \triangleq D_{\text{req}}$ . This leads to the maximum value of the target average latency, which is denoted as

$$D_{\text{req}} = \mathbb{E}[T_n]_{\text{max}} = (1 - \Gamma_n)e_n. \quad (21)$$

Subtracting the bandwidth-independent fixed delays  $T_{\text{fixed}} = T_i^{\text{sense}} + T_{i,n}^{\text{compute}} + T_n^{\text{control}}$ , the communication budget is denoted as  $T_{\text{budget}} = D_{\text{req}} - T_{\text{fixed}}$ . Therefore, the bandwidth  $\kappa_i$  must satisfy  $S_i/(\kappa_i \log_2(1 + \text{SNR}_{i,n})) \leq T_{\text{budget}}$ , i.e.,

$$\kappa_i \geq \frac{S_i}{T_{\text{budget}} \log_2(1 + \text{SNR}_{i,n})}, \quad (22)$$

completing the proof.  $\square$

Therefore, the constraint (17a) of **Problem 1** can be reconstructed as  $\kappa_i \geq \kappa_i^{\min}$ . Considering the above analysis, we can derive the optimization problem of the UAV as

$$\begin{aligned} \text{Problem 1 : } \max_{\varrho_n} U_n^L &= \sum_{i \in \mathcal{M}_n} \beta_{i,n} (\varrho_n - c_n) \kappa_i, \\ \text{s.t. } \kappa_i &\geq \frac{S_i}{T_{\text{budget}} \log_2(1 + \text{SNR}_{i,n})}, \end{aligned} \quad (23a)$$

$$\sum_{i \in \mathcal{M}_n} \kappa_i \leq \kappa_n^{\text{total}}. \quad (23b)$$

2) *Utilities of Users:* Each user  $i$  seeks to maximize its information gain while minimizing the payment to the UAV. The follower's utility function is formulated as

$$U_i^F = \sum_{n \in \mathcal{N}} \beta_{i,n} (\vartheta_i \ln(1 + \kappa_i H_{i,n}) - \varrho_n \kappa_i), \quad \forall i \in \mathcal{I}, \quad (24)$$

where  $H_{i,n} = \log_2(1 + \text{SNR}_{i,n})$  is the spectral efficiency, and  $\vartheta_i$  is the urgency weight representing the user's demand. The utility function is composed of the revenue obtained from the transmitted data minus the price that needs to be paid for the UAV. Furthermore, the optimization problem of users is denoted as follows:

$$\begin{aligned} \text{Problem 2 : } \max_{\kappa_i} U_i^F \\ &= \sum_{n \in \mathcal{N}} \beta_{i,n} (\vartheta_i \ln(1 + \kappa_i H_{i,n}) - \varrho_n \kappa_i), \\ \text{s.t. } \sum_{n \in \mathcal{N}} \beta_{i,n} &= 1. \end{aligned} \quad (25)$$

This constraint ensures that the user can select at most one UAV for information transmission. From a control-theoretic perspective, a unique feedback link prevents the reception of conflicting control commands from multiple UAVs, ensuring the stability and convergence of the tracking loop.

3) *Backward Induction Method:* To determine the Stackelberg equilibrium, we employ the backward induction method, starting with the followers' subgame. For a given pricing strategy  $\varrho_n$ , the first-order and second-order derivatives of the user's utility  $U_i^F$  with respect to its bandwidth demand  $\kappa_i$  are derived as

$$\frac{\partial U_i^F}{\partial \kappa_i} = \frac{\vartheta_i H_{i,n}}{1 + \kappa_i H_{i,n}} - \varrho_n, \quad \frac{\partial^2 U_i^F}{\partial \kappa_i^2} = -\frac{\vartheta_i (H_{i,n})^2}{(1 + \kappa_i H_{i,n})^2} < 0. \quad (26)$$

Since the second-order derivative is strictly negative, the utility function  $U_i^F$  is strictly concave with respect to the bandwidth demand  $\kappa_i$  [37]. This ensures that the user's optimization problem is well-posed and possesses a unique global maximum. Consequently, the optimal bandwidth request can be uniquely determined by solving the first-order condition, i.e.,  $\frac{\partial U_i^F}{\partial \kappa_i} = 0$ . We derive the closed-form expression for the best response strategy  $\kappa_i^*$  of user  $i$  as

$$\kappa_i^* = \frac{\vartheta_i}{\varrho_n} - \frac{1}{H_{i,n}}. \quad (27)$$

Let  $\sum_{i \in \mathcal{M}_n} \vartheta_i = \Theta$ , and  $\sum_{i \in \mathcal{M}_n} \frac{1}{H_{i,n}} = H_n$ . Substitute the user's optimal strategy into the UAV's utility function, the **Problem 1** can be reconstructed as follows:

$$\begin{aligned} \text{Problem 1 : } \max_{\varrho_n} U_n^L &= (\varrho_n - c_n) \left( \frac{\Theta}{\varrho_n} - H_n \right), \\ \text{s.t. } \varrho_n &\leq \frac{\vartheta_i}{\kappa_i^{\min} + \frac{1}{H_{i,n}}} = \bar{\varrho}_n, \end{aligned} \quad (28a)$$

$$\varrho_n \geq \frac{\Theta}{\kappa_n^{\text{total}} + H_n} = \underline{\varrho}_n. \quad (28b)$$

The derivatives of the utility function  $U_n^L$  of UAV  $n$  with respect to the price strategy  $\varrho_n$  up to the first and second orders are provided as

$$\frac{\partial U_n^L}{\partial \varrho_n} = -H_n + \frac{c_n \Theta}{\varrho_n^2}, \quad \frac{\partial^2 U_n^L}{\partial \varrho_n^2} = -\frac{2c_n \Theta}{\varrho_n^3} < 0. \quad (29)$$

The strict concavity of the UAV's utility function  $U_n^L$  is guaranteed by  $\frac{\partial^2 U_n^L}{\partial \varrho_n^2} < 0$ , ensuring the existence of a unique optimal pricing strategy [38]. By solving the first-order condition, we obtain the unconstrained optimal price  $\varrho_n^1 = \sqrt{\frac{c_n \Theta}{H_n}}$ . Considering the constraints in **Problem 1**, the final optimal price  $\varrho_n^*$  is determined by projecting  $\varrho_n^1$  onto the feasible interval  $[\underline{\varrho}_n, \bar{\varrho}_n]$ , leading to the following three cases.

- 1) **Constraints not activated:** If  $\underline{\varrho}_n \leq \varrho_n^1 \leq \bar{\varrho}_n$ , the unconstrained solution is feasible. In this case,  $\varrho_n^* = \varrho_n^1$ , which harmonizes profit maximization with both system stability and capacity limits.
- 2) **Stability constraint activated:** If  $\varrho_n^1 > \bar{\varrho}_n$ , the stability constraint becomes activated. To ensure that the bandwidth requested by users remains sufficient to satisfy the Lyapunov stability requirement, the UAV must cap its price at  $\varrho_n^* = \bar{\varrho}_n$ , prioritizing system convergence over marginal profit.
- 3) **Capacity constraint activated:** If  $\varrho_n^1 < \underline{\varrho}_n$ , the capacity constraint is activated. To prevent system congestion and ensure that the aggregate bandwidth request does not exceed the total capacity of the UAV  $\kappa_n^{total}$ , the UAV must set its price to the lower limit  $\varrho_n^* = \underline{\varrho}_n$  to suppress excessive demand.

Therefore, the optimal response strategy  $\varrho_n^*$  for UAV  $n$  is expressed as

$$\varrho_n^* = \begin{cases} \underline{\varrho}_n, & \text{if } \sqrt{\frac{c_n \Theta}{H}} < \underline{\varrho}_n, \\ \sqrt{\frac{c_n \Theta}{H}}, & \text{if } \underline{\varrho}_n \leq \sqrt{\frac{c_n \Theta}{H}} \leq \bar{\varrho}_n, \\ \bar{\varrho}_n, & \text{if } \sqrt{\frac{c_n \Theta}{H}} > \bar{\varrho}_n. \end{cases} \quad (30)$$

#### IV. ALGORITHM FOR STRATEGIES DESIGN

It is challenging to solve the proposed Stackelberg game in a dynamic environment presents significant challenges due to the hierarchical interactions and the high dimensionality of the solution space. While DRL offers a potent framework for decision-making under uncertainty, deploying traditional DRL models on UAVs is often impractical [11]. UAVs are characterized by limited on-board energy and computing resources, making the execution of large-scale neural networks computationally prohibitive. To address the challenge, we formulate the interaction between UAVs (leaders) and users (followers) as a Multi-Agent Markov Decision Process (MAMDP). Furthermore, we introduce a pruning-based PPO algorithm, which integrates structural pruning with the PPO framework to significantly compress the network architecture, enabling rapid convergence to the Stackelberg equilibrium with minimal computational overhead.

##### A. MAMDP Formulation for the Stackelberg Game

The stochastic interaction is formulated as a MAMDP, defined by the tuple  $M_n = \{\mathcal{S}_n, \mathcal{A}_n, \mathcal{P}_n, \mathcal{R}_n, \gamma_n\}$  for each UAV  $n$  [11], representing the state space, action space, transition probability, reward function, and discount factor, respectively. In this framework, UAVs operate as independent agents optimizing pricing strategies based on partial observations. To

mitigate the non-stationarity inherent in multi-agent environments, an experience replay mechanism with buffer capacity  $L$  is employed. The core components are defined as follows.

1) *Observation Space:* Due to privacy constraints and limited communication bandwidth, UAVs cannot access the global state of the system. Instead, each UAV  $n$  constructs a local observation  $\mathbf{s}_n(t)$  at time step  $t$ , where  $\mathcal{S}_n \triangleq \{\mathbf{s}_n(t)\}$ .  $\mathbf{s}_n(t)$  encapsulates the current status and a temporal window of historical interactions to capture the users' reaction patterns. Specifically,  $\mathbf{s}_n(t)$  consists of the pricing history and the corresponding aggregate bandwidth demands from the associated users  $\mathcal{M}_n$  over the previous  $L$  time steps:

$$\mathbf{s}_n(t) = \{\varrho_n(\tau), \kappa_n(\tau) \mid \tau \in [t-L, t-1]\}, \quad (31)$$

where  $\kappa_n(\tau) = \sum_{i \in \mathcal{M}_n} \kappa_i(\tau)$  represents the total bandwidth requested by users covered by UAV  $n$ .

2) *Action Space:* The action space  $\mathcal{A}_n$  corresponds to the decision variable of the leader in the Stackelberg game. Based on the local observation  $\mathbf{s}_n(t)$ , the UAV agent determines its pricing strategy. Therefore, the action at time  $t$  is denoted as  $a_n(t) = \varrho_n(t)$ , where  $\varrho_n(t)$  represents the unit price for bandwidth resources and  $\mathcal{A}_n \triangleq \{\varrho_n(t)\}$ .

3) *Reward Function:* The reward signal  $\mathcal{R}_n$  drives the learning process, guiding the UAV toward optimal policy formulation. Upon executing action  $\varrho_n(t)$  and observing the users' response, the environment returns an immediate reward  $r_n(t)$ , where  $\mathcal{R}_n \triangleq \{r_n(t)\}$ . To align the learning objective with the game-theoretic goal, the reward is defined as the utility function of the UAV leader, i.e.,  $r_n(t) = a \times U_n^L(\varrho_n(t))$ , where  $a > 0$  ensures numerical stability without altering the optimal policy structure. The agent seeks to maximize the expected cumulative discounted reward  $\mathbb{E} [\sum_{k=0}^{\infty} \gamma_n^k r_n(t+k)]$ , where  $\gamma_n$  is the discount factor [39].

##### B. Proposed Pruning-based PPO Algorithm

To achieve efficient strategy updates on resource-constrained UAVs, we propose a compact DRL scheme based on the actor-critic architecture. Unlike traditional methods that utilize fully connected dense networks, our pruning-based PPO algorithm dynamically eliminates redundant neural connections during the training phase [8].

1) *PPO-based Optimization Objective:* We adopt the Multi-Agent PPO (MAPPO) as the backbone due to its stability in continuous action spaces. The architecture comprises an actor network, which is parameterized by  $\theta_n$ , representing the policy  $\pi_{\theta_n}(\varrho_n | \mathbf{s}_n)$ , and a critic network, which is parameterized by  $\omega_n$ , estimating the value function  $V_{\omega_n}(\mathbf{s}_n)$ . To ensure monotonic improvement, the objective function for the actor network is formulated using a clipped surrogate objective, which is denoted as  $L_{\text{actor}}(\theta_n) = \mathbb{E} [\min (\rho_n(\theta_n) \hat{A}_n, \text{clip}(\rho_n(\theta_n), 1-\varphi, 1+\varphi) \hat{A}_n)]$ , where  $\rho_n(\theta_n) = \frac{\pi_{\theta_n}(\varrho_n | \mathbf{s}_n)}{\pi_{\theta_n^{\text{old}}}(\varrho_n | \mathbf{s}_n)}$  denotes the probability ratio between the new and old policies, and  $\varphi$  is a hyperparameter controlling the clipping range to prevent drastic policy updates.

The advantage function  $\hat{A}_n$  is estimated via the Generalized Advantage Estimation (GAE) method, which is shown as

$$\hat{A}_n(\mathbf{s}_n, \varrho_n) = \sum_{l=0}^{\infty} (\gamma_n \lambda)^l \delta_n(t+l), \quad (32)$$

where  $\delta_n(t) = r_n(t) + \gamma_n V_{\omega_n}(\mathbf{s}_n(t+1)) - V_{\omega_n}(\mathbf{s}_n(t))$  is the Temporal Difference (TD) error.

2) *Dynamic Structural Pruning*: To reduce the computational load, we incorporate a structured pruning mechanism directly into the actor network. Let the actor network consist of  $H$  layers. We introduce a binary mask matrix  $\mathbf{m}^{(h)} \in \{0, 1\}$  for the  $h$ -th layer, which acts as a gatekeeper for neuronal activation [40]. If a neuron's contribution is below a dynamic threshold,  $\mathbf{m}^{(h)}$  sets its output to zero, effectively removing it from the computational graph. The sparsified output of the  $h$ -th layer is expressed as

$$\varrho_n(t) = \nu_n^{(H)} \left( \theta_n^{(H)} \mathbf{o}_n^{(H-1)} * \mathbf{m}_n^{(H)} \right), \quad (33)$$

where  $\nu_n^{(H)}$  and  $\mathbf{o}_n^{(H-1)}$  correspond to the nonlinear response and the input vector of the output  $H$ -th layer, respectively. The symbol  $*$  denotes the Hadamard product [41]. Consequently, the optimization objective  $L_{\text{actor}}$  depends on both the network weights and the mask structure, i.e.,  $L_{\text{actor}}(\theta_n, \mathbf{m})$ .

During the training phase, the parameters are updated iteratively. The actor network weights  $\theta_n$  are optimized via gradient ascent to maximize the clipped objective, while the critic network weights  $\omega_n$  are updated via gradient descent to minimize the value estimation error [8], which are respectively calculated as

$$\theta_n^{(h)} \leftarrow \theta_n^{(h)} - l_n^1 \frac{\partial L_{\text{actor}}(\theta_n, \mathbf{m})}{\partial \left( \theta_n^{(h)} \mathbf{o}_n^{(h)} * \mathbf{m}_n^{(h)} \right)} \cdot \frac{\partial \left( \theta_n^{(h)} \mathbf{o}_n^{(h)} * \mathbf{m}_n^{(h)} \right)}{\partial \theta_n^{(h)}}, \quad (34)$$

$$\omega_n^{(h)} \leftarrow \omega_n^{(h)} - l_n^2 \frac{\partial L_{\text{critic}}(\omega_n)}{\partial \omega_n}, \quad (35)$$

where  $l_n^1$  and  $l_n^2$  denote the respective learning rates. By iteratively refining the policy and the sparsity mask, the UAVs converge to an optimal pricing strategy that approximates the Stackelberg equilibrium while maintaining a lightweight network footprint [42].

3) *Pruning-based PPO via Dynamic Structured Pruning*: To ensure the proposed MADRL framework is computationally lightweight and suitable for deployment, we incorporate a dynamic structured pruning mechanism. Unlike unstructured methods, which may lead to irregular memory access, structured pruning reduces model complexity by systematically discarding superfluous neurons and their associated connections. The pruning procedure is governed by an iterative evaluation of neuronal significance, primarily consisting of two phases, i.e., calculation of a time-variant threshold and the updating of a binary activation mask [43]. Specifically, the dynamic pruning threshold  $\phi(t)$  at time step  $t$  is formulated as

$$\phi(t) = \sum_{j=1}^J \sum_{h=1}^H n_j^{(h)} \cdot w(t), \quad (36)$$

---

**Algorithm 1** Pruning-based PPO Algorithm via Dynamic Pruning for the Stackelberg Game

---

```

1: Input: Initial observation  $\mathbf{s}_n(0)$  for each UAV  $n$ , learning
   rates  $l_n^1, l_n^2$ , clip parameter  $\varphi$ , discount  $\gamma_n$ , and pruning
   parameters  $w_1, w_2, t_0, M, \nabla$ .
2: Initialization: Initialize actor parameters  $\theta_n$ , critic parameters  $\omega_n$ , and binary mask  $\mathbf{m}_n^{(h)}$ .
3: for episode  $k = 1, 2, \dots, K_{\max}$  do
4:   // Phase 1: MAMDP Interaction & Data Collection
5:   for time step  $t = 1, \dots, T_{\text{step}}$  do
6:     UAV  $n$  observes local state  $\mathbf{s}_n(t)$  via Eq. (31).
7:     Generate pricing action  $\varrho_n(t)$  using the masked
       policy based on Eq. (33).
8:     Execute  $\varrho_n(t)$ , receive reward  $r_n(t)$ , and observe
       next state  $\mathbf{s}_n(t+1)$ .
9:     Store transition tuple in replay buffer  $\mathcal{D}$ .
10:    end for
11:   // Phase 2: PPO-based Policy Optimization
12:   Calculate Advantage  $\hat{A}_n(\mathbf{s}_n, \varrho_n)$  via GAE in Eq. (32).
13:   Update Critic parameters  $\omega_n$  as
14:      $\omega_n^{(h)} \leftarrow \omega_n^{(h)} - l_n^2 \nabla_{\omega_n} L_{\text{critic}}(\omega_n)$  by Eq. (35).
15:   Update Actor parameters  $\theta_n$  as
16:      $\theta_n^{(h)} \leftarrow \theta_n^{(h)} - l_n^1 \nabla_{\theta_n} L_{\text{actor}}(\theta_n, \mathbf{m})$  by Eq. (34).
17:   // Phase 3: Dynamic Structured Pruning
18:   if pruning condition met (e.g.,  $k > t_0$ ) then
19:     Update target sparsity  $w(k)$  via cubic decay as
       shown in Eq. (37).
20:     Calculate neuron importance  $n_j^{(h)}$  for layer  $h$ .
21:     Compute dynamic threshold  $\phi(k)$  via Eq. (36).
22:     Update mask  $\mathbf{m}_n$  for each neuron  $j$  in layer  $h$ 
       based on Eq. (38).
23:     Apply mask to parameters:  $\theta_n \leftarrow \theta_n * \mathbf{m}_n$ .
24:   end if
25: end for
26: Output: The optimal policy  $\pi_{\theta_n^*}$  and mask  $\mathbf{m}_n^*$ .

```

---

where  $n_j^{(h)}$  quantifies the importance score of the  $j$ -th neuron in the  $h$ -th layer, and  $J$  denotes the total number of layers. The term  $w(t)$  represents the target sparsity level, which evolves over the training process. To achieve a smooth transition from a dense network to a compact one, we employ a cubic decay schedule for the sparsity ratio  $w(t)$ , which is expressed as

$$w(t) = w_1 + (w_1 - w_2) \left( 1 - \frac{t - t_0}{M \nabla t} \right)^3, \quad (37)$$

where  $w_1$  and  $w_2$  correspond to the initial and target sparsity densities, respectively. The parameters  $t_0$ ,  $M$ , and  $\nabla$  denote the pruning start epoch, the total number of pruning iterations, and the pruning frequency, respectively. Based on these metrics, the algorithm identifies and retains only the most significant neurons. A binary mask  $m_j^{(h)}$  is utilized to enforce pruning physically, i.e., if a neuron's importance metric falls below the threshold  $\phi$ , it is deactivated. The mask update rule is defined as

$$m_j^{(h)} = \begin{cases} 1, & \text{if } \text{abs} \left| m_j^{(h)}, \theta_j^{(h)} \right| \geq \phi, \\ 0, & \text{otherwise.} \end{cases} \quad (38)$$

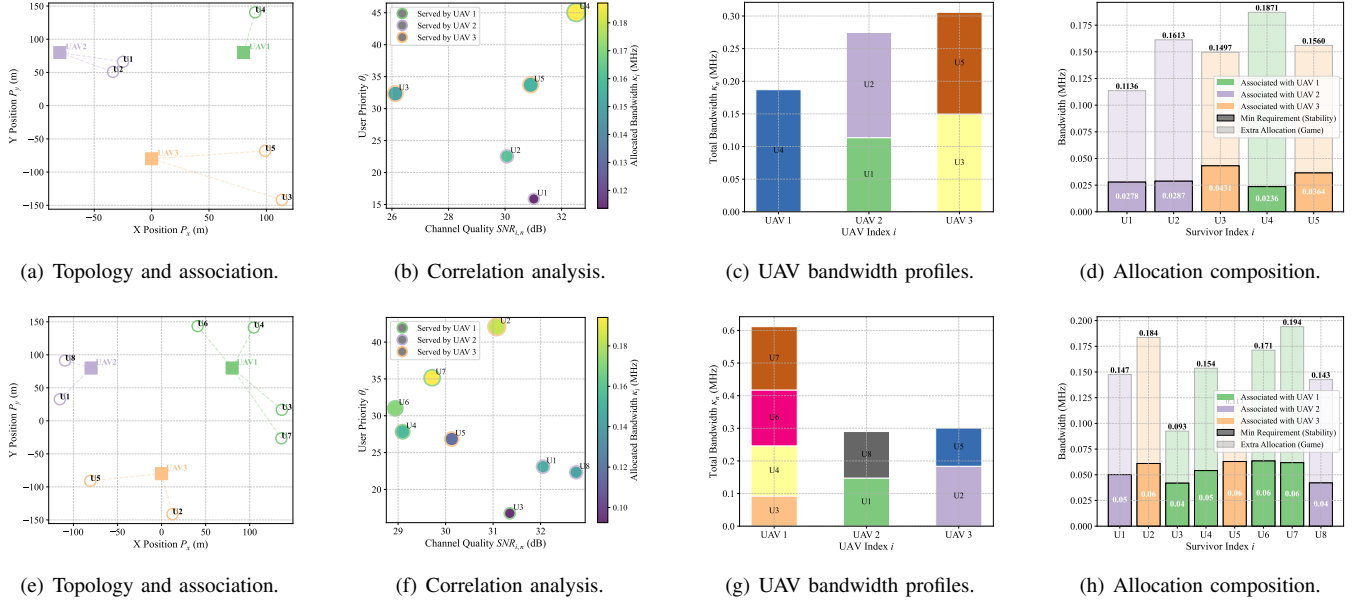


Fig. 2: Comparative analysis of network topology and bandwidth allocation strategies under different load conditions. The top row (a)-(d) presents the scenario with 3 UAVs and 5 users, while the bottom row (e)-(h) depicts the scenario with 3 UAVs and 8 users. The columns illustrate: (a/e) spatial distribution and association; (b/f) correlation between bandwidth, channel quality, and priority; (c/g) aggregate bandwidth usage per UAV; and (d/h) decomposition into stability-required and utility-maximizing bandwidth.

where  $\theta_j^{(h)}$  represents the associated network parameters. This mechanism ensures that the model progressively converges to an optimal, lightweight structure while maintaining learning performance. The proposed framework integrates the PPO architecture with a dynamic structured pruning mechanism to achieve a lightweight yet robust policy. As outlined in **Algorithm 1**, the optimization process follows a coarse-to-fine paradigm, i.e., the agent first undergoes a preliminary training phase to establish a baseline policy, which is subsequently refined by iteratively excising redundant nodes from the actor-critic networks. We further analyze the computational overhead of this scheme. The total algorithmic complexity over  $T$  episodes is bounded by  $\mathcal{O}(TO) + \mathcal{O}\left(T \sum_{h=1}^{H-1} v^{(h)}\right)$  [8], representing the processing costs associated with the observation dimension  $O$  and the cumulative operations of  $v^{(h)}$  neurons across the hidden layers, respectively.

## V. NUMERICAL RESULTS

In this section, we present numerical results to validate the effectiveness and theoretical consistency of the proposed Stackelberg game-based resource management framework. Similar to the experimental setups in [8], [44], the key system parameters are summarized in Table I.

Fig. 2 provides a comprehensive validation of the proposed Stackelberg game-based management scheme, specifically analyzing user association dynamics and resource allocation under varying load conditions (5 users versus 8 users), where  $U_i$  in the figure represents the user with index  $i$ . Figs. 2(a) and 2(e) visualize the topological association based on channel quality. The results reveal a distinct spatial clustering phenomenon, where users are dynamically associated with proximal UAVs to mitigate path loss. Within the SC

TABLE I: Simulation Parameters and Hyperparameters Setting.

Parameters	Values
Target sampling period ( $e_n$ )	0.5 s
Required CPU cycles per bit ( $f_0$ )	1000 cycles
Computational capabilities of UAV ( $f_n$ )	1 GHz
Total bandwidth of UAV $n$ ( $\kappa_n^{total}$ )	[15, 25] MHz
User transmit power ( $P_i$ )	[100, 300] mW
User data packet size ( $S_i$ )	[40, 64] kbytes
Reference channel gain ( $h_0$ )	-40 dB
Additive white Gaussian noise ( $\sigma^2$ )	-100 dBm
Lyapunov decay rate ( $\rho_n$ )	0.95
Control time constant ( $\tau_n$ )	0.005 s
Maximum unit price constraint ( $\varrho_{max}$ )	5
User emergency weight ( $\vartheta_i$ )	[1.0, 5.0]
Epoch	500
Step per epoch	200
Learning rate	$1 \times 10^{-3}$
Discount factor	0.95
GAE lambda	0.95
Clip parameter	0.2
Mini-batch size	32
Hidden layer units	[256, 256]

framework, this proximity-aware association is critical for minimizing propagation latency, thereby preserving the timeliness of the sensing-control loop. In addition, Figs. 2(b) and 2(f) elucidate the determinants of bandwidth allocation by correlating allocated resources with SNR and user priority. A robust positive correlation is observed that users served by the same UAV who exhibit critical physical states (indicated by higher urgency weights) or superior channel conditions secure a larger share of the spectrum. This corroborates that the proposed pricing mechanism effectively prioritizes

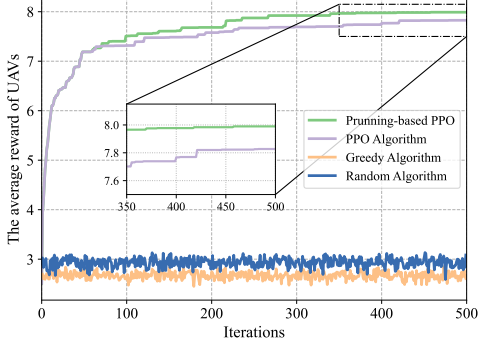


Fig. 3: Test reward comparison of the proposed pruning-based PPO algorithm with other algorithms, i.e., PPO, greedy, and random algorithms.

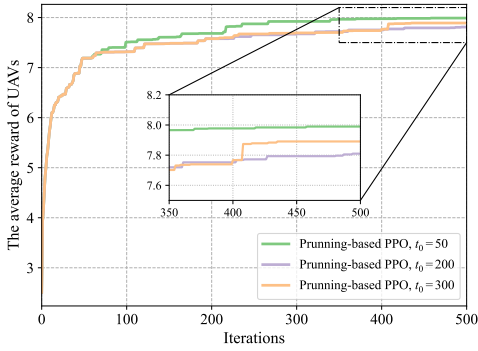
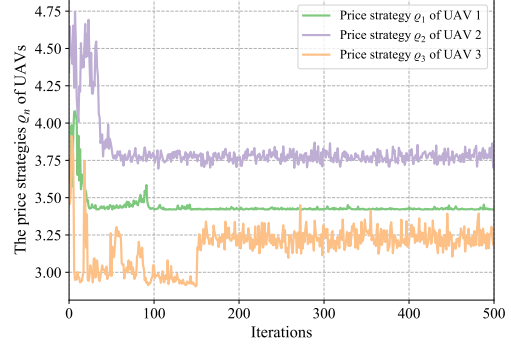


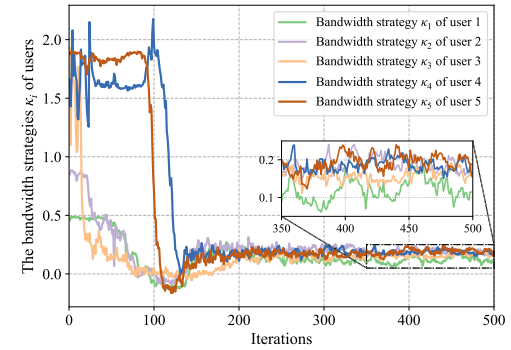
Fig. 4: Test reward comparison of the proposed pruning-based PPO algorithm with other algorithms in different pruning epochs.

vulnerable nodes, ensuring high-frequency state updates for targets with the most urgent control requirements. From a system stability perspective, Figs. 2(c) and 2(g) quantify the aggregate bandwidth utilization across the UAV fleet, demonstrating effective load balancing. Moreover, Figs. 2(d) and 2(h) provide a decomposition of the allocated bandwidth into stability-oriented and utility-oriented components for each user. The “min requirement” denotes the hard lower bound derived via Lyapunov optimization, which is necessary to guarantee the probabilistic stability of the physical control loop. It can be observed that the actual allocated bandwidth strictly supersedes this theoretical threshold for all users. This result confirms that the proposed strategy successfully enforces physical system stability as a baseline constraint while enabling users to acquire surplus bandwidth to maximize their individual satisfaction.

Fig. 3 evaluates the learning efficiency of the proposed pruning-based algorithm against standard PPO and baseline benchmarks (i.e., greedy and random algorithms). While the baselines stagnate at low reward levels, both PPO variants demonstrate robust convergence. Notably, the proposed pruning-based PPO achieves a superior asymptotic reward compared to the standard PPO. This suggests that the structured pruning mechanism acts as a regularizer, removing redundant parameters that contribute to overfitting. By focusing on essential state features, the agent derives a more efficient



(a) Pricing strategies of UAVs



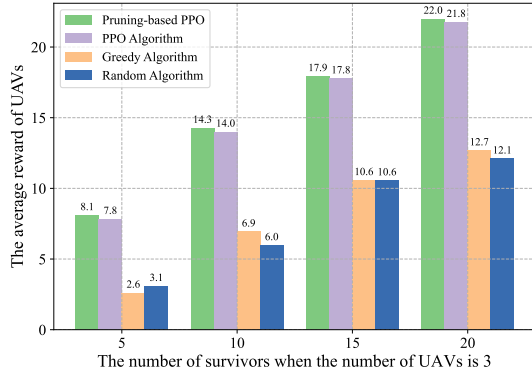
(b) Bandwidth request strategies of users.

Fig. 5: Stackelberg strategies of UAVs and users are output by the proposed pruning-based PPO algorithm.

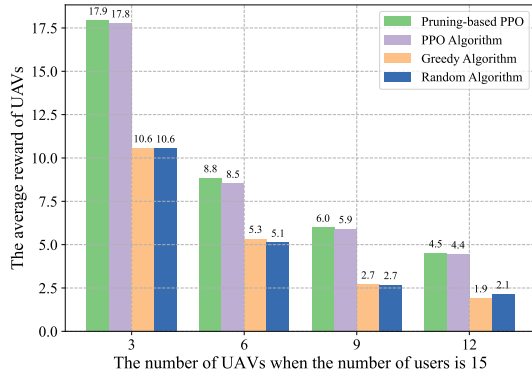
policy for UAV decision-making, ensuring robust control feedback even under the noise of dynamic LAE environments.

Fig. 4 investigates the impact of pruning start epoch  $t_0$  on performance over 500 epochs. A non-monotonic relationship is observed, i.e., early intervention ( $t_0 = 50$ ) yields the highest convergence reward, followed by late intervention ( $t_0 = 300$ ), while intermediate settings ( $t_0 = 200$ ) perform suboptimally. Initiating pruning early allows the agent to co-adapt its policy with the sparse topology from the outset, effectively acting as a regularizer that filters out environmental noise and prevents overfitting to redundant features. Conversely, late pruning serves as robust model compression on a mature policy, preserving the strong baseline established during the dense training phase. However, pruning during the critical policy formation phase disrupts the learning inertia, leading to structural instability that is difficult to recover from. Consequently, these results demonstrate that early structural intervention is the optimal strategy for the proposed pruning-based PPO framework, enabling the UAV to maximize decision-making utility while maintaining a lightweight architecture throughout the majority of the learning process.

Fig. 5 illustrates the evolutionary trajectory of the strategic interactions between the UAVs (i.e., leaders) and users (i.e., followers) throughout the iterations. Specifically, Fig. 5(a) depicts the dynamic adjustment of the UAVs’ pricing strategies. In the initial phase, the pricing curves exhibit



(a) Test reward comparison of the proposed pruning-based PPO with other algorithms when the number of users is different.



(b) Test reward comparison of the proposed pruning-based PPO with other algorithms when the number of UAVs is different.

Fig. 6: Test reward comparison of the proposed pruning-based PPO algorithm with other algorithms when the number of UAVs or users is different.

significant oscillations as the agent explores the action space to identify the optimal incentive mechanism. However, as the iterations proceed, the pricing strategies gradually stabilize and converge to steady values. Correspondingly, Fig. 5(b) presents the adaptive bandwidth requests of the users. In response to the varying pricing signals from the UAVs, users dynamically adjust their resource demands to maximize their individual utilities based on their specific urgency weights. Consequently, the convergence of both pricing and bandwidth strategies demonstrates that the system successfully reaches a stable Stackelberg equilibrium. At this equilibrium point, neither the leader nor the followers can improve their utility by unilaterally deviating from their current strategies, thereby validating the convergence guarantee and theoretical feasibility of the proposed pruning-based PPO algorithm.

Fig. 6 investigates the impact of varying node densities on the system performance, illustrating how the UAV reward fluctuates with the number of users and UAVs. Specifically, Fig. 6(a) plots the reward evolution with the number of users ranging from 5 to 20, while the number of UAVs is fixed at 3. We can observe that as the number of users increases, the reward obtained by the UAVs rises significantly. This indicates that the proposed mechanism effectively incentivizes UAVs to serve a larger population, i.e., a higher density of users

translates to more service requests and, consequently, greater cumulative average rewards. Conversely, Fig. 6(b) examines the scenario where the number of users is fixed at 15, while the number of UAVs varies from 3 to 12. In this case, the average reward per UAV exhibits a downward trend as the fleet size increases. This phenomenon reflects market saturation, where an oversupply of resources reduces the equilibrium price and individual revenue. These trends confirm that the proposed model correctly captures the economic principles of the Stackelberg game while adapting to the physical scale of the mission.

## VI. CONCLUSION

This paper investigates the critical integration of resource allocation and control stability in the LAE scenario through a unified SC<sup>3</sup> closed-loop framework. By leveraging Lyapunov stability theory, we have explicitly mapped physical control requirements to communication constraints, transforming the stability problem into a quantifiable Stackelberg game that balances heterogeneous user demands. To enable real-time execution on resource-constrained UAVs, we have proposed a pruning-based PPO algorithm utilizing dynamic structured pruning to approximate the game equilibrium. Simulation results confirm that the proposed scheme significantly enhances system utility and ensures robust control stability in dynamic LAE environments, compared with existing baselines. For future work, we will model and analyze composite end-to-end latency fluctuations arising from jointly time-varying energy and bandwidth resources, and deepen the control-communication synergy by investigating bidirectional co-design mechanisms.

## REFERENCES

- [1] Z. Tian, L. Wang, L. Xu, C. Xu, and A. Fei, "Coded caching for reliable map dissemination in symbiotic communication aided emergency UAV systems," *IEEE Transactions on Cognitive Communications and Networking*, vol. 10, no. 5, pp. 1663–1677, 2024.
- [2] A. Fotouhi, H. Qiang, M. Ding, M. Hassan, L. G. Giordano, A. Garcia-Rodriguez, and J. Yuan, "Survey on UAV cellular communications: Practical aspects, standardization advancements, regulation, and security challenges," *IEEE Communications surveys & tutorials*, vol. 21, no. 4, pp. 3417–3442, 2019.
- [3] X. Zhou, J. Xiong, H. Zhao, C. Yan, H. Wang, and J. Wei, "Population-invariant MADRL for AoI-aware UAV trajectory design and communication scheduling in wireless sensor networks," *IEEE Internet of Things Journal*, vol. 12, no. 3, pp. 2545–2561, 2025.
- [4] H. Jin, W. Yuan, J. Wu, J. Wang, D. Niyato, X. Wang, G. K. Karagiannidis, Z. Lin, Y. Gong, D. I. Kim *et al.*, "Advancing the control of low-altitude wireless networks: architecture, design principles, and future directions," *npj Wireless Technology*, vol. 2, no. 1, p. 2, 2026.
- [5] G. Sun, L. He, Z. Sun, Q. Wu, S. Liang, J. Li, D. Niyato, and V. C. Leung, "Joint task offloading and resource allocation in aerial-terrestrial UAV networks with edge and fog computing for post-disaster rescue," *IEEE Transactions on Mobile Computing*, vol. 23, no. 9, pp. 8582–8600, 2024.
- [6] H. Jin, J. Wu, W. Yuan, F. Liu, and Y. Cui, "Co-design of sensing, communications, and control for low-altitude wireless networks," *arXiv preprint arXiv:2506.20970*, 2025.
- [7] T. Wang, S. Wang, X. Lan, Y. Liu, Q. Chen, and P. Xiao, "On the AoI-aware status update in buffer-aided wireless-powered internet of things network," *IEEE Internet of Things Journal*, vol. 11, no. 7, pp. 12551–12566, 2024.
- [8] J. Kang, Y. Zhong, M. Xu, J. Nie, J. Wen, H. Du, D. Ye, X. Huang, D. Niyato, and S. Xie, "Tiny multiagent DRL for twins migration in UAV metaverses: A multileader multifollower stackelberg game approach," *IEEE Internet of Things Journal*, vol. 11, no. 12, pp. 21021–21036, 2024.

[9] Q. Wang, Z. Li, M. Chen, H. Zhao, and H. Zhu, "Optimizing dynamic spectrum sharing in UAV-assisted networks: Hybrid two-stage stackelberg game approach," *IEEE Internet of Things Journal*, vol. 12, no. 19, pp. 40 517–40 530, 2025.

[10] Y. Tong, J. Chen, M. Xu, J. Kang, Z. Xiong, D. Niyato, C. Yuen, and Z. Han, "Multi-attribute auction-based resource allocation for twins migration in vehicular metaverses: A GPT-based DRL approach," *IEEE Transactions on Cognitive Communications and Networking*, vol. 11, no. 1, pp. 638–654, 2025.

[11] K. Chung, C. Lee, and Y. Tsang, "Neural combinatorial optimization with reinforcement learning in industrial engineering: a survey," *Artificial Intelligence Review*, vol. 58, no. 5, p. 130, 2025.

[12] X. Ye, Y. Mao, X. Yu, S. Sun, L. Fu, and J. Xu, "Integrated sensing and communications for low-altitude economy: A deep reinforcement learning approach," *IEEE Transactions on Wireless Communications*, vol. 25, pp. 351–367, 2026.

[13] B. Hu, H. Liu, J. Du, M. López-Benítez, C. Wu, X. Chu, and D. Niyato, "MADQN-enhanced computation offloading and resource allocation for 6G low-altitude economy vehicular networks," *IEEE Transactions on Cognitive Communications and Networking*, vol. 12, pp. 2603–2617, 2026.

[14] R. Chai, K. Chen, B. Hua, Y. Lu, Y. Xia, X.-M. Sun, G.-P. Liu, and W. Liang, "A two phases multiobjective trajectory optimization scheme for multi-UGVs in the sight of the first aid scenario," *IEEE Transactions on Cybernetics*, vol. 54, no. 9, pp. 5078–5091, 2024.

[15] Y. Wan, Y. Zhong, A. Ma, and L. Zhang, "An accurate UAV 3-D path planning method for disaster emergency response based on an improved multiobjective swarm intelligence algorithm," *IEEE Transactions on Cybernetics*, vol. 53, no. 4, pp. 2658–2671, 2023.

[16] Y. Guo, Y. Chen, H. Li, Y. Wu, and J. Huang, "AoI-aware incentive mechanism for UAV-assisted mobile crowdsensing: A contract-theoretic approach," *IEEE Transactions on Mobile Computing*, vol. 25, no. 2, pp. 1660–1677, 2026.

[17] Q. Wang, Y. Shen, L. Xu, H. Zhang, H. Zhao, and H. Zhu, "Optimizing spectrum sharing in UAV swarms: A stackelberg game-based incentive mechanism," *IEEE Transactions on Vehicular Technology*, vol. 75, no. 1, pp. 1443–1454, 2026.

[18] G. Sun, L. He, Z. Sun, Q. Wu, S. Liang, J. Li, D. Niyato, and V. C. M. Leung, "Joint task offloading and resource allocation in aerial-terrestrial UAV networks with edge and fog computing for post-disaster rescue," *IEEE Transactions on Mobile Computing*, vol. 23, no. 9, pp. 8582–8600, 2024.

[19] Z. Liu, D. Niyato, J. Wang, G. Sun, L. Huang, Z. Gao, and X. Wang, "Generative AI for lyapunov optimization theory in UAV-based low-altitude economy networking," *IEEE Network*, pp. 1–9, 2026.

[20] H. Yang, H. Zhang, F. Luo, F. Liu, and H. Chen, "Pruning-based deep reinforcement learning for task offloading in end-edge-cloud collaborative mobile edge computing," *Journal of Computing and Electronic Information Management*, vol. 13, no. 1, pp. 1–9, 2024.

[21] Z. Li, W. Su, M. Xu, R. Yu, D. Niyato, and S. Xie, "Compact learning model for dynamic off-chain routing in blockchain-based IoT," *IEEE Journal on Selected Areas in Communications*, vol. 40, no. 12, pp. 3615–3630, 2022.

[22] K. Roth, O. Vinyals, and Z. Akata, "Non-isotropy regularization for proxy-based deep metric learning," in *Proceedings of the IEEE/CVF conference on computer vision and pattern recognition*, 2022, pp. 7420–7430.

[23] B. Karaman, I. Basturk, S. Taskin, E. Zeydan, F. Kara, E. A. Beyazit, M. Camelo, E. Björnson, and H. Yanikomeroglu, "Solutions for sustainable and resilient communication infrastructure in disaster relief and management scenarios," *IEEE Communications Surveys & Tutorials*, vol. 28, pp. 716–760, 2026.

[24] A. Khan, S. Gupta, and S. K. Gupta, "Emerging UAV technology for disaster detection, mitigation, response, and preparedness," *Journal of Field Robotics*, vol. 39, no. 6, pp. 905–955, 2022.

[25] B. Chang, L. Zhang, L. Li, G. Zhao, and Z. Chen, "Optimizing resource allocation in URLLC for real-time wireless control systems," *IEEE Transactions on Vehicular Technology*, vol. 68, no. 9, pp. 8916–8927, 2019.

[26] G. Pechlivanidou and N. Karampetakis, "Zero-order hold discretization of general state space systems with input delay," *IMA Journal of Mathematical Control and Information*, vol. 39, no. 2, pp. 708–730, 2022.

[27] P. Park, S. Coleri Ergen, C. Fischione, C. Lu, and K. H. Johansson, "Wireless network design for control systems: A survey," *IEEE Communications Surveys & Tutorials*, vol. 20, no. 2, pp. 978–1013, 2018.

[28] A. Komae, "Dynamic gain adaptation in linear quadratic regulators," *IEEE Transactions on Automatic Control*, vol. 69, no. 8, pp. 5094–5108, 2023.

[29] Y. Long, S. Gong, S. Sun, G. C. F. Lee, L. Li, and D. Niyato, "Lyapunov-guided deep reinforcement learning for semantic-aware AoI minimization in UAV-assisted wireless networks," *IEEE Transactions on Wireless Communications*, vol. 24, no. 8, pp. 6351–6364, 2025.

[30] H. Wang, A. Liu, and N. N. Xiong, "SGCS: A cost-effective quality control system for strategic workers in mobile crowd sensing," *IEEE Transactions on Network Science and Engineering*, vol. 12, no. 2, pp. 1146–1158, 2025.

[31] X. Liu, L. Lv, and Q. Yang, "LEO-satellite-assisted UAV path optimization for space-air-ground internet of remote things networks," *Space: Science & Technology*, vol. 5, p. 0280, 2025.

[32] M. Ren, L. Qiao, L. Yang, Z. Gao, J. Chen, M. B. Mashhadi, P. Xiao, R. Tafazolli, and M. Bennis, "Generative semantic communication via textual prompts: Latency performance tradeoffs," *IEEE Transactions on Vehicular Technology*, vol. 74, no. 9, pp. 14 843–14 848, 2025.

[33] P. Fard Moshiri, M. Simsek, and B. Kantarcı, "Joint optimization of completion ratio and latency of offloaded tasks with multiple priority levels in 5G edge," *IEEE Transactions on Network and Service Management*, vol. 22, no. 2, pp. 1357–1371, 2025.

[34] K. Ogata, *Modern control engineering*. Prentice hall, 2010.

[35] Q. Miao, K. Zhang, and B. Jiang, "Fixed-time collision-free fault-tolerant formation control of multi-UAVs under actuator faults," *IEEE Transactions on Cybernetics*, vol. 54, no. 6, pp. 3679–3691, 2024.

[36] S. M. Ross, *Introduction to probability and statistics for engineers and scientists*. Academic press, 2020.

[37] J. Liu, M. Xiao, J. Wen, J. Kang, R. Zhang, T. Zhang, D. Niyato, W. Zhang, and Y. Liu, "Optimizing resource allocation for multi-modal semantic communication in mobile AIGC networks: A diffusion-based game approach," *IEEE Transactions on Cognitive Communications and Networking*, vol. 11, no. 5, pp. 3346–3360, 2025.

[38] Y. Zhong, J. Wen, J. Zhang, J. Kang, Y. Jiang, Y. Zhang, Y. Cheng, and Y. Tong, "Blockchain-assisted twin migration for vehicular metaverses: A game theory approach," *Transactions on Emerging Telecommunications Technologies*, vol. 34, no. 12, p. e4856, 2023.

[39] J. Huang, R. Zhou, M. Li, H. Li, Y. Liu, and X. Song, "From black-box to white-box: Interpretable deep reinforcement learning with kolmogorov-arnold networks for autonomous driving," *Transportation Research Part C: Emerging Technologies*, vol. 182, p. 105386, 2026.

[40] W. Su, Z. Li, M. Xu, J. Kang, D. Niyato, and S. Xie, "Compressing deep reinforcement learning networks with a dynamic structured pruning method for autonomous driving," *IEEE Transactions on Vehicular Technology*, vol. 73, no. 12, pp. 18 017–18 030, 2024.

[41] G. G. Chrysos, Y. Wu, R. Pascanu, P. H. Torr, and V. Cevher, "Hadamard product in deep learning: Introduction, advances and challenges," *IEEE Transactions on Pattern Analysis and Machine Intelligence*, vol. 47, no. 8, pp. 6531–6549, 2025.

[42] Y. Wei, Z. Zeng, Y. Zhong, J. Kang, R. W. Liu, and M. S. Hossain, "Bi-LSTM based multi-agent DRL with computation-aware pruning for agent twins migration in vehicular embodied AI networks," *arXiv preprint arXiv:2505.06378*, 2025.

[43] J. Wen, J. Kang, D. Niyato, Y. Zhang, and S. Mao, "Sustainable diffusion-based incentive mechanism for generative AI-driven digital twins in industrial cyber-physical systems," *IEEE Transactions on Industrial Cyber-Physical Systems*, vol. 3, pp. 139–149, 2025.

[44] X. Peng, X. Lan, and Q. Chen, "Age-of-task-aware AAV-based mobile edge computing techniques in emergency rescue applications," *IEEE Internet of Things Journal*, vol. 12, no. 7, pp. 8909–8930, 2025.